

# Internal Cation Mobilities and their Isotope Effects in the Molten System (Li, K)Cl

Arnold Lundén

Department of Physics, Chalmers University of Technology, S-41296 Göteborg, Sweden

Isao Okada

Department of Electronic Chemistry, Tokyo Institute of Technology at Nagatsuta, Yokohama, Japan\*

Z. Naturforsch. **41 a**, 1034–1040 (1986); received May 13, 1986

With the Klemm method, the internal mobility ratios of the Li and K,  $^6\text{Li}$  and  $^7\text{Li}$ , and  $^{39}\text{K}$  and  $^{41}\text{K}$  have been measured for melts of the system (Li, K)Cl near the eutectic composition (ca. 56% Li) in the range 729–976 K. Under all these conditions the Chemla effect occurs, i.e.  $b_{\text{Li}} < b_{\text{K}}$  ( $b$ : internal mobility). In the region near the anode the composition becomes that corresponding to the Chemla crossing point, which shifts with temperature toward higher concentration of  $\text{Li}^+$ . Both  $b_{\text{Li}}$  and  $b_{\text{K}}$  have been found to be well expressed by the equation  $b = [A/(V - V_0)] \exp(-E/RT)$  ( $V$ : molar volume,  $A$  and  $E$ : constants depending on the respective cation,  $V_0$ : a parameter depending on the respective cation and temperature), which is also valid for the mobilities in alkali nitrates when the Coulombic attraction plays a dominant role. The isotope effects of both cations seem to be similar to those in pure LiCl and KCl and slightly increase with temperature.

## Introduction

It has been shown for molten nitrates that internal mobility data of binary nitrates are more informative than those of pure nitrates for the understanding of the ionic transport [1]. In many additive binary molten salts with two univalent cations the Chemla effect [2] occurs. Its interpretation may be the key to a better understanding of the mechanism of ionic transport in molten salts.

Alkali chlorides are the most typical and simple salts, and therefore we have chosen the (Li, K)Cl system in this study, which is also among the most useful ones from a practical viewpoint. Although the melting points of mixtures of halides are higher than those of nitrates, a wide temperature range can be covered. The isotope effects of the internal mobilities have also been determined and compared with those of the pure salts, i.e. LiCl and KCl.

Ratios of the internal mobilities of the present system had been determined with the Hittorf method [3] and the Klemm method [4]; the former experiments were done around 913 K and the latter

at relatively low temperature (700–778 K). Smirnov et al. measured the ratio in the systems (Li, K)Cl, (Li, Cs)Cl, (Na, K)Cl and (Na, Cs)Cl with the EMF method [5] and regarded it as temperature-independent, overlooking the previous findings mentioned in such papers as [6, 7] that the mobility ratios of two cations in an additive binary mixture are generally temperature-dependent.

We have employed the Klemm method, i.e., a countercurrent electromigration method, which is the most accurate one for the present purpose.

One of our experiments has already been reported in a previous paper [8] in order to demonstrate an anomalous isotope distribution in a separation tube containing a binary mixture such as the present one.

## Experimental

The chemicals LiCl and KCl were of reagent grade. The salts were dried at 120 °C overnight, mixed in a prescribed ratio and melted. No attempt was made to remove remaining traces of moisture, since the Klemm method is insensitive to its presence in the separation tube.

An electromigration cell is shown in Figure 1. A portion of the melt was stored in a small vessel,

\* Nagatsuta 4259, Midori-ku, Yokohama 227, Japan.

Reprint requests to Professor A. Lundén, Department of Physics, Chalmers University of Technology, S-41296 Göteborg, Sweden.

0340-4811 / 86 / 0800-1034 \$ 01.30/0. – Please order a reprint rather than making your own copy.



Dieses Werk wurde im Jahr 2013 vom Verlag Zeitschrift für Naturforschung in Zusammenarbeit mit der Max-Planck-Gesellschaft zur Förderung der Wissenschaften e.V. digitalisiert und unter folgender Lizenz veröffentlicht: Creative Commons Namensnennung-Keine Bearbeitung 3.0 Deutschland Lizenz.

Zum 01.01.2015 ist eine Anpassung der Lizenzbedingungen (Entfall der Creative Commons Lizenzbedingung „Keine Bearbeitung“) beabsichtigt, um eine Nachnutzung auch im Rahmen zukünftiger wissenschaftlicher Nutzungsformen zu ermöglichen.

This work has been digitalized and published in 2013 by Verlag Zeitschrift für Naturforschung in cooperation with the Max Planck Society for the Advancement of Science under a Creative Commons Attribution-NoDerivs 3.0 Germany License.

On 01.01.2015 it is planned to change the License Conditions (the removal of the Creative Commons License condition “no derivative works”). This is to allow reuse in the area of future scientific usage.

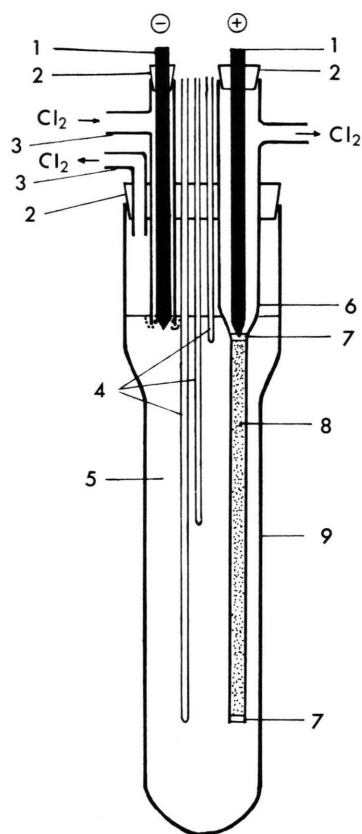


Fig. 1. Electromigration cell. 1: Carbon electrode, 2: Silicone stopper, 3: Vycor tube, 4: sheath for C. A. thermocouple, 5: molten (Li, K)Cl near the eutectic composition, 6: separation tube (i.d.: 4 mm, length: ca. 20 cm), 7: quartz wool, 8: quartz powder (100–150 mesh), 9: quartz vessel.

from which the melt was filled into a separation tube before each run of electromigration, since the salt in the large vessel could become contaminated after several runs of electromigration. Both electrodes were carbon rods. Chlorine gas, which was dried by passing through conc. sulfuric acid, was bubbled into the melt around the cathode in order to convert otherwise electrodeposited metal into the chloride. The conversion was smooth above ca. 490 °C.

In most runs the temperature was kept at the respective average value within  $\pm 8$  °C; the vertical temperature distribution in the melt was also nearly within this range.

After electromigration, the separation tube was taken out, thoroughly cleaned on the outside wall, and cut into pieces of ca. 1.5 cm (corresponding to

ca. 100 mg of salt) for chemical analysis and mass spectrometric analysis. The salt in each piece was dissolved in distilled water, and after taking out the quartz powder, the solution was diluted to 100 cm<sup>3</sup>. From this 2 cm<sup>3</sup> were taken and diluted to 100 cm<sup>3</sup> for chemical analysis; for Li<sup>+</sup> and K<sup>+</sup> ions atomic absorption and emission spectrometry was employed, respectively. The total amount of the cations in each fraction was also checked a few times by titrating the H<sup>+</sup> ions eluted from a cation exchanger (Dowex 50 W-X 8) column charged with another portion of the solution.

## Results

The main experimental conditions and the results are given in Tables 1 and 2. The  $\varepsilon_c$ ,  $\varepsilon_{Li}$ , and  $\varepsilon_K$  are defined as

$$\varepsilon_c = (b_{Li} - b_K)/\bar{b}, \quad (1a)$$

$$\varepsilon_{Li} = (b_6 - b_7)/b_{Li}, \quad (1b)$$

$$\varepsilon_K = (b_{39} - b_{41})/b_K, \quad (1c)$$

where  $b$  is internal mobility;  $\bar{b} = x_{Li} b_{Li} + x_K b_K$  ( $x$ : mole fraction,  $x_{Li} + x_K = 1$ ),  $b_{Li} = y_6 b_6 + y_7 b_7$  and  $b_K = y_{39} b_{39} + y_{41} b_{41}$  ( $y$ : abundance of the isotopes, i.e.,  $y_6 + y_7 = 1$  and  $y_{39} + y_{41} = 1$ ); suffixes 6, 7, 39 and 41 refer to <sup>6</sup>Li<sup>+</sup>, <sup>7</sup>Li<sup>+</sup>, <sup>39</sup>K<sup>+</sup> and <sup>41</sup>K<sup>+</sup> ions, respectively. These values were calculated according to the equations in [8, 9].

The average composition in a few fractions near the anode is given as  $x_{Li}^c$  in Table 1. In the first fraction, which included salt sticking to the inner wall of the separation tube around the anode, the concentration was rather irregular, probably because of evaporation. Meanwhile in the next few fractions, the concentrations were virtually constant, the averaged value of which is given.

In all the runs an anomalous distribution of the lithium isotopes was observed along the separation tube. The zone next to the anode, where <sup>7</sup>Li is enriched, was immediately followed by a region where a slight but distinct enrichment of <sup>6</sup>Li occurred, whereas <sup>41</sup>K was enriched in both these regions. A typical example of the distribution of the isotopes was given in [8].

Table 1. Conditions and results.  $Q$  is the transported charge; for the other symbols, see the text. The sign  $\pm$  for  $\varepsilon_c$ ,  $\varepsilon_{Li}$  and  $\varepsilon_K$  stands for the standard deviation resulting from errors of one series of chemical and mass spectrometric analysis; it does not include the errors of the reproducibility.

$x_{Li}^a$	$T/K$	$Q/C$	$x_{Li}^c$	$\varepsilon_c$	$\varepsilon_{Li}$	$\varepsilon_K$
0.560	729	8585	0.617	$-0.0846 \pm 0.0072$	$0.0148 \pm 0.0001$	$0.00106 \pm 0.00003$
0.560	747	10223	0.679	$-0.0715 \pm 0.0052$	$0.0110 \pm 0.0001$	$0.00194 \pm 0.00002$
0.560	773	10457	0.713	$-0.0800 \pm 0.0046$	$0.0153 \pm 0.0001$	$0.00154 \pm 0.00001$
0.560	792	11233	0.707	$-0.105 \pm 0.005$	$0.0202 \pm 0.0001$	$0.00257 \pm 0.00001$
0.560	806	11247	0.726	$-0.134 \pm 0.006$	$0.0214 \pm 0.0001$	$0.00117 \pm 0.00001$
0.595 <sup>b</sup>	828	6275	0.756	$-0.138 \pm 0.005$	$0.0141 \pm 0.0003$	$0.00358 \pm 0.00023$
0.560	847	12468	0.766	$-0.117 \pm 0.005$	$0.0203 \pm 0.0001$	$0.00141 \pm 0.00001$
0.560	868	12334	0.783	$-0.145 \pm 0.005$	$0.0176 \pm 0.0001$	$0.00128 \pm 0.00001$
0.560	911	8755	—	$-0.175 \pm 0.010$	$0.0171 \pm 0.0001$	$0.00250 \pm 0.00025$
0.560	913	13549	0.786	$-0.101 \pm 0.004$	$0.0150 \pm 0.0001$	$0.00059 \pm 0.00001$
0.560	937	12020	0.810	$-0.0780 \pm 0.0049$	$0.0149 \pm 0.0001$	$0.00279 \pm 0.00003$
0.560	941	12641	0.802	$-0.133 \pm 0.004$	$0.0197 \pm 0.0001$	$0.00113 \pm 0.00001$
0.595	976	5182	0.791	$-0.162 \pm 0.004$	$0.0175 \pm 0.0001$	$0.00458 \pm 0.00004$

<sup>a</sup> The maximum error may be  $\pm 0.01$ .

<sup>b</sup> For this run, the chemical and isotope distribution in the separation tube is given in Table 1 of [8].

Table 2. Internal mobilities of  $Li^+$  and  $K^+$  ions in the (Li, K)Cl mixtures. The sign  $\pm$  for  $b_{Li}$  and  $b_K$  stands for the standard deviation resulting from that of only  $\varepsilon_c$  and  $x_{Li}$ .

$x_{Li}$	$T/K$	$\alpha/S \text{ cm}^{-1} \text{ a}$	$V/\text{cm}^3 \text{ mol}^{-1} \text{ a}$	$b_{Li}/10^{-8} \text{ m}^2 \text{ V}^{-1} \text{ s}^{-1}$	$b_K/10^{-8} \text{ m}^2 \text{ V}^{-1} \text{ s}^{-1}$
0.560	729	1.515	34.31	$5.19 \pm 0.02$	$5.64 \pm 0.02$
0.560	747	1.628	34.50	$5.64 \pm 0.01$	$6.05 \pm 0.02$
0.560	773	1.785	34.80	$6.21 \pm 0.02$	$6.73 \pm 0.02$
0.560	792	1.895	35.01	$6.56 \pm 0.02$	$7.28 \pm 0.02$
0.560	806	1.973	35.19	$6.77 \pm 0.02$	$7.73 \pm 0.03$
0.595	828	2.199	34.85	$7.50 \pm 0.02$	$8.59 \pm 0.02$
0.560	847	2.190	35.67	$7.68 \pm 0.02$	$8.62 \pm 0.02$
0.560	868	2.294	35.92	$8.00 \pm 0.02$	$9.23 \pm 0.02$
0.560	911	2.491	36.46	$8.69 \pm 0.05$	$10.33 \pm 0.06$
0.560	913	2.500	36.48	$9.03 \pm 0.02$	$9.98 \pm 0.02$
0.560	937	2.600	36.79	$9.36 \pm 0.03$	$10.61 \pm 0.04$
0.560	941	2.616	36.84	$9.40 \pm 0.02$	$10.74 \pm 0.03$
0.595	976	2.841	36.53	$10.05 \pm 0.03$	$11.79 \pm 0.03$

<sup>a</sup> Data taken from [12].

## Discussion

The temperature-dependence of  $\varepsilon_c$  near the eutectic composition is shown in Fig. 2, the  $\varepsilon_c$  values obtained by the previous studies [3, 4] also being shown for comparison; the agreement is good.

Under the experimental conditions the Chemla effect occurred ( $\varepsilon_c < 0$ ). The measured final composition around the anode  $x_{Li}^c$  is plotted against temperature in Figure 3. Note that the composition at the anode must in the long run become that corresponding to the Chemla crossing point [10]. In Fig. 3,  $x_{Li}^c$  values obtained in other studies [3, 4] are also plotted. Besides, the  $x_{Li}^c$  value at 1100 K can be estimated to be 0.90 from Fig. 4b in [5]. Kanno [11]

has reported two experiments at 973 K on (Li, K)Cl melts with the initial compositions of 67 and 33 mol% of LiCl. The composition had changed in the whole separation column, and no calculations can be made of the elementary separation factors  $\varepsilon_c$ ,  $\varepsilon_{Li}$ , and  $\varepsilon_K$ , but for both experiments the highest concentration of Li obtained near the anode is ca. 0.8. Thus, our values are in good agreement with the others.

In Fig. 4, isotherms of  $b_{Li}$  and  $b_K$  are shown; data on conductivity and molar volume needed for these calculations are taken from [12]. It should be noted that the slopes of the isotherms for  $b_{Li}$  are considerably steeper than those in binary alkali nitrates but somewhat less steep than those in (Li, K)<sub>2</sub>CO<sub>3</sub> [13].

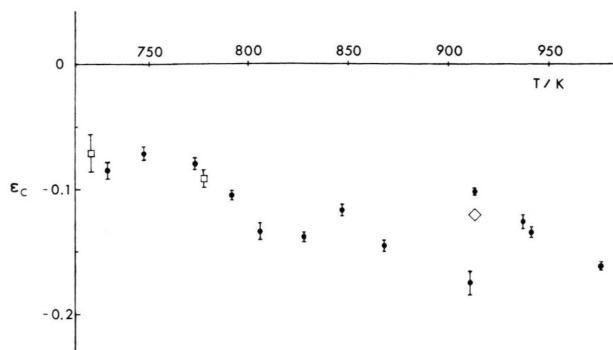


Fig. 2. Relative differences in internal mobilities,  $\varepsilon_c = (b_{\text{Li}} - b_{\text{K}})/b$ , near the eutectic composition.  $\diamond$ : ref. [3],  $\square$ : ref. [4].

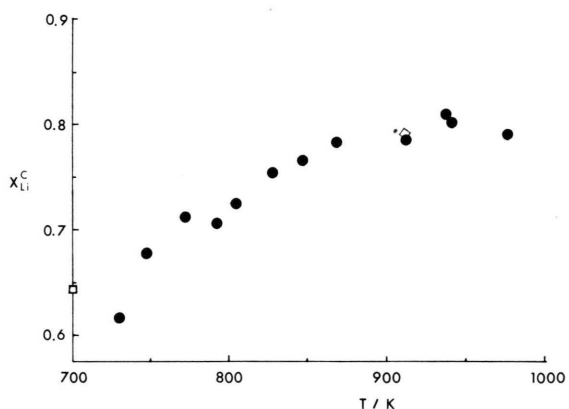


Fig. 3. Reached composition near the anode, corresponding to the Chemla crossing point, vs. temperature.  $\diamond$ : ref. [3],  $\square$ : ref. [4].

Thus, this difference may be attributed to that in the Coulombic attraction between cation and anion rather than to that in the shapes of the anions, since the shapes of nitrate and carbonate ions are very similar. As the Coulombic attraction between unlike ions is stronger, an increase of the average distance between neighbouring anions will result in a more substantial increase of the potential barrier for a cation moving from one anion toward another.

In the present system the composition near the anode becomes soon that of the Chemla crossing point because the slopes of the isotherms of the two cations differ considerably.

As seen from Figs. 3 and 4, the Chemla crossing point shifts with increasing temperature toward higher concentrations of the smaller cation, as is

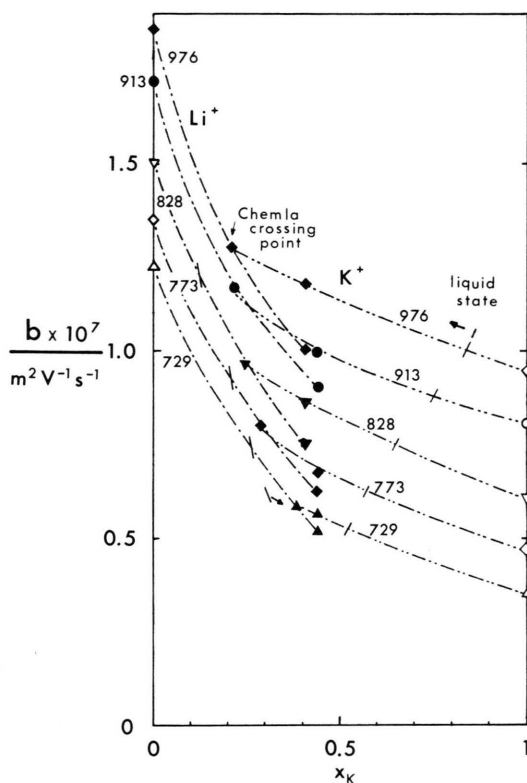


Fig. 4. Mobility isotherms of  $\text{Li}^+$  and  $\text{K}^+$ . The figures in the drawing denote temperatures in K. The open marks refer to fictive melts obtained by extrapolation of the data in [12] with respect to temperature.

always observed with the Chemla effect. This can be explained in a similar way as in the composition-dependence of the isotherms of cation internal mobilities stated above. As a cation is smaller, the Coulombic attraction part of the pair potential curve with the counter anion is steeper. Therefore, an increase of the average distances between neighbouring anions caused by a temperature increase will give rise to a steeper barrier for a smaller cation than for a larger one to move away from the nearest neighbouring anion. In other words, with increasing temperature the association of a smaller cation increases faster than that of the larger one [14]. Thus,  $b_{\text{Li}}/b_{\text{K}}$  decreases with temperature.

In case that the Coulombic attraction between unlike ions is the dominant factor influencing the relative magnitudes of cationic mobilities [15], the internal mobilities of the cations of binary mixtures of alkali nitrates have been found to be well

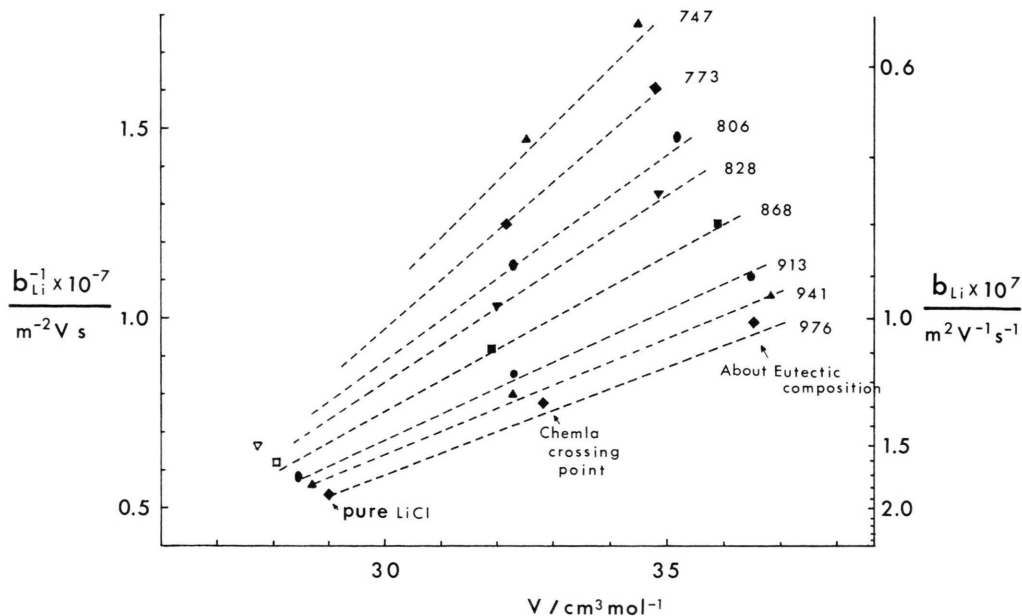


Fig. 5. Reciprocals of the internal mobilities of  $\text{Li}^+$  vs. molar volume. The broken lines are drawn according to (2) with the parameter values of Table 3. See also the legend of Figure 4.

expressed by the equation

$$b = [A/(V - V_0)] \exp(-E/RT), \quad (2)$$

where  $A$  and  $E$  are constants depending on the respective cation,  $V$  is the molar volume of the mixture and  $V_0$  is a constant nearly independent of temperature.

We have tried to fit the  $b_{\text{Li}}$  and  $b_{\text{K}}$  values in the present system to (2). The parameter values thus obtained are given in Table 3. In order to show the  $V$  dependence explicitly,  $b_{\text{Li}}^{-1}$  and  $b_{\text{K}}^{-1}$  are plotted vs.  $V$  at several temperatures in Figs. 5 and 6, respectively.

As seen from Fig. 5,  $b_{\text{Li}}$  seems to be well expressed by (2) with the parameter values of Table 3; at low temperature and, particularly, at high concentration of LiCl,  $b_{\text{Li}}$  is smaller than expected from (2), presumably because the effective free space is too small. This had been observed also for  $b_{\text{Li}}$  in alkali nitrate mixtures at high concentrations of  $\text{LiNO}_3$  [15].  $V_0$  seems to be dependent on temperature, whereas in molten nitrates it is virtually temperature-independent [16].  $V$  at the Chemla crossing point is nearly independent of temperature, as seen from Fig. 5, because  $V$  increases with  $T$  at constant  $x_{\text{Li}}$  but decreases with  $x_{\text{Li}}^{\text{C}}$ , the latter increasing with  $T$ .

Table 3. Parameter values for  $b$  in (2).

	$A/10^{-10} \text{ m}^5 \text{ V}^{-1} \cdot \text{s}^{-1} \text{ mol}^{-1}$	$E/\text{kJ mol}^{-1}$	$V_0/10^{-6} \text{ m}^3 \text{ mol}^{-1}$
$b_{\text{Li}}$	0.4858	26.62	$35.54 - 0.0169 (T/\text{K})$
$b_{\text{K}}$	6.080	38.86	$99.16 - 0.1079 (T/\text{K})$

The  $b_{\text{K}}$  values of the fictive melts of pure KCl in Fig. 6 have been obtained through extrapolations of the data at higher temperatures [12]. As seen from Fig. 6,  $b_{\text{K}}$  can also be expressed in the form of (2), except at lower temperatures, where the effective free space is too small. In the case of  $(\text{Li, K})\text{NO}_3$ , however, the values of the parameters of (2) are somewhat different from those for such mixtures as  $(\text{K, Rb})\text{NO}_3$  and  $(\text{K, Cs})\text{NO}_3$ , for which the Coulombic attraction effect is the dominant factor for  $b_{\text{K}}$ . The agitation effect and the free space effect should be included in the equation for  $b_{\text{K}}$  in the present case. This will be clarified when  $b_{\text{K}}$  is measured in such systems as  $(\text{K, Rb})\text{Cl}$  and  $(\text{K, Cs})\text{Cl}$ . In the present case  $V_0$  seems to be strongly dependent on the temperature, which is in contrast to the case of nitrates.

As stated in Results, an anomalous distribution of the  $\text{Li}^+$  isotopes was observed in all the runs. The

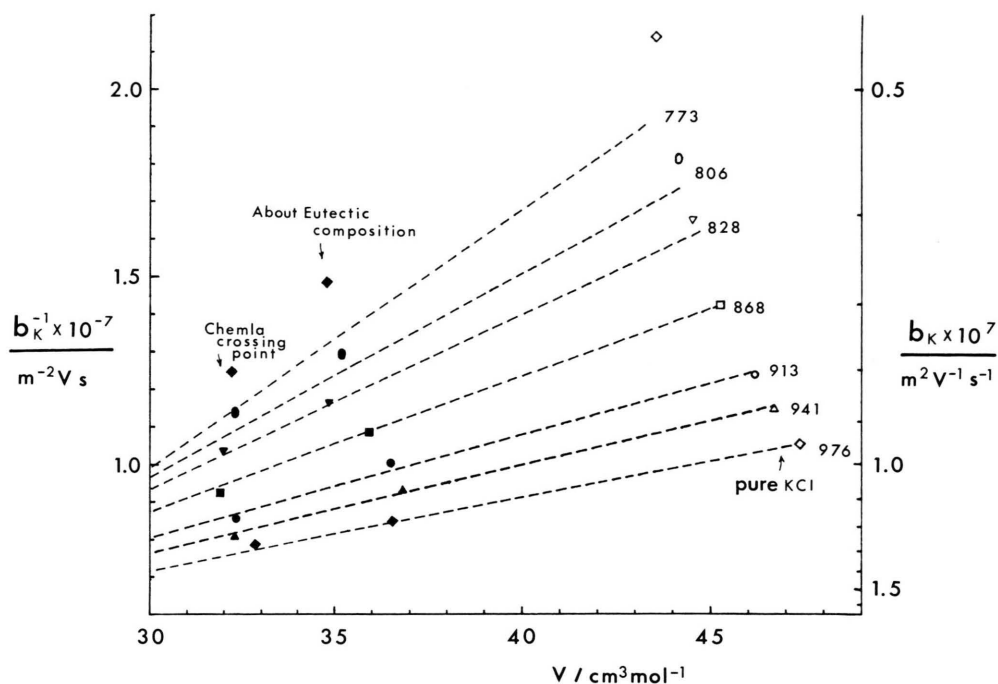


Fig. 6. The reciprocal of internal mobilities of  $K^+$  ions vs. molar volume. See also the legend of Figure 4.

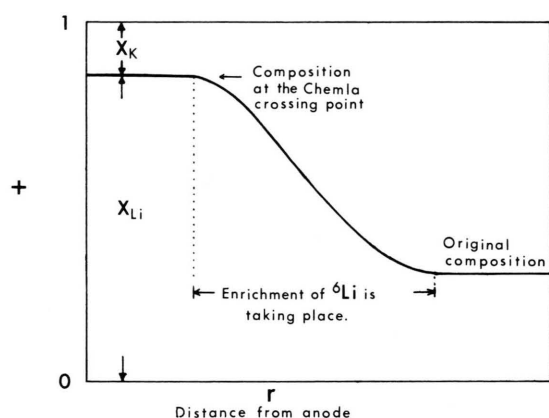


Fig. 7. Schematic representation of a distribution of the chemical composition after some time of electromigration.

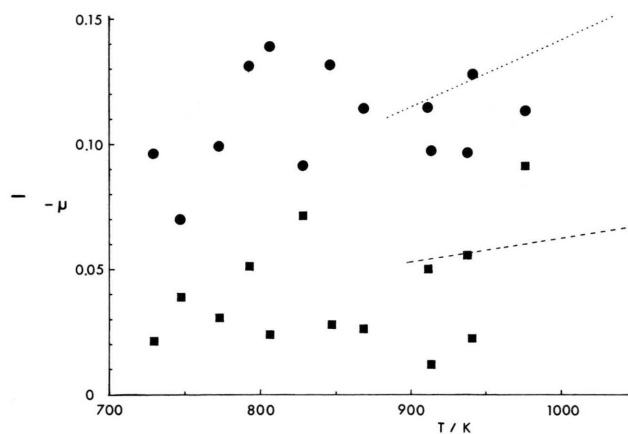


Fig. 8. The mass effect of  $Li^+$  and  $K^+$  in the mixture. ●:  $Li^+$ , ■:  $K^+$ . The dotted and broken lines show the extrapolated values for pure LiCl [18] and KCl [19], respectively.

distribution of the chemical composition in the separation tube after some time of electromigration is schematically shown in Figure 7. Enrichment of  $^6Li$  is to take place in the region where  $dx_{Li}/dr < 0$ , although enriched  $^7Li$  at the anode is diffusing into

some part of this region near the anode. This was discussed in detail in the previous paper [8].

The temperature dependence of the isotope effect for  $Li^+$  and  $K^+$  ions in the mixture, expressed as the mass effect [17], is compared with that for pure

LiCl [18] and KCl [19] in Fig. 8; the mass effect  $\mu$  is defined as  $\epsilon_{\text{Li(K)}}$  divided by the relative mass difference [17]. The data scatter mainly because of errors in mass spectrometric measurements. However, the following may be mentioned.

It is evident that  $\mu_{\text{Li}}$  is greater than  $\mu_{\text{K}}$  at every temperature. It seems that the mass effects in the present mixture are more or less consistent with the extrapolation for the pure salts, although the present temperature range is far below that for pure LiCl (993–1173 K) [18] and KCl (1093–1293 K) [19]. The temperature-dependence of the mass effects of  $\text{Li}^+$  in the present system seems to be small, if any;

this is in contrast to that in the (Li, K) $\text{NO}_3$  mixture of the eutetic composition, where both  $\mu_{\text{Li}}$  and  $\mu_{\text{K}}$  clearly increase with temperature [20]. For the main purpose of studying the chemical and isotope effect of the internal mobilities, molecular dynamics simulation has been done for the present system [21]. A detailed discussion concerning the isotope effect will be given there.

We are indebted to Mr. M. Lövenby for mass spectrometric analysis and to the Swedish Natural Science Research Council and Chalmersska Forskningsfonden for financial support of the work in Göteborg.

- [1] See Table I in R. Takagi, K. Kawamura, and I. Okada, *Z. Naturforsch.* **39a**, 759 (1984).
- [2] J. Périé and M. Chemla, *C.R. Acad. Sci. Paris* **250**, 3986 (1960).
- [3] C. T. Moynihan and R. W. Laity, *J. Phys. Chem.* **68**, 3312 (1964).
- [4] R. Takagi, H. Shimotake, and K. J. Jensen, *J. Electrochem. Soc.* **131**, 1280 (1984).
- [5] M. V. Smirnov, K. A. Aleksandrov, and V. A. Khokhlov, *Electrochim. Acta* **22**, 543 (1977).
- [6] F. Lantelme and M. Chemla, *Bull. Soc. Chim. Fr.* **1963**, 2200.
- [7] K. Kawamura, I. Okada, and O. Odawara, *Z. Naturforsch.* **30a**, 69 (1975).
- [8] I. Okada and A. Lundén, *Z. Naturforsch.* **38a**, 97 (1983). — Equations (32) and (33) of this paper contain erroneously the concentration  $c$ . They have to be replaced by the corresponding molar amounts.
- [9] V. Ljubimov and A. Lundén, *Z. Naturforsch.* **21a**, 1592 (1966).
- [10] F. Lantelme and M. Chemla, *J. Chim. Phys.* **60**, 250 (1963).
- [11] H. Kanno, *J. Nucl. Sci. Technol.* **7**, 42 (1970).
- [12] G. J. Janz, R. P. T. Tomkins, C. B. Allen, J. R. Downey Jr., G. L. Gardner, U. Krebs, and S. K. Singer, *J. Phys. Chem. Ref. Data* **4**, 871 (1975).
- [13] C. Yang, I. Okada, R. Takagi, and K. Kawamura, unpublished.
- [14] A. Klemm, *Z. Naturforsch.* **39a**, 471 (1984).
- [15] C. Yang, R. Takagi, and I. Okada, *Z. Naturforsch.* **38a**, 135 (1983).
- [16] C. Yang, R. Takagi, and I. Okada, *Z. Naturforsch.* **35a**, 1186 (1980).
- [17] A. Klemm, H. Hintenberger, and P. Hoernes, *Z. Naturforsch.* **2a**, 245 (1947).
- [18] S. Jordan, R. Lenke, and A. Klemm, *Z. Naturforsch.* **23a**, 1563 (1968).
- [19] S. Jordan and A. Klemm, *Z. Naturforsch.* **21a**, 1584 (1966).
- [20] A. Lundén, J. Habasaki, and I. Okada, unpublished.
- [21] I. Okada, to be published.